HHS Public Access

Author manuscript

Ann N Y Acad Sci. Author manuscript; available in PMC 2021 May 21.

Published in final edited form as:

Ann N Y Acad Sci. 2021 April ; 1490(1): 77–89. doi:10.1111/nyas.14568.

Progranulin Promotes Bone Fracture Healing via TNFR pathways in Mice with Type 2 Diabetes Mellitus

Yuanjing Ding[#a,b], **Jianlu Wei**[#a,c], **Aubryanna Hettinghouse**[a], **Guangfei Li**[a], **Xin Li**[d], **Thomas A. Einhorn**[a], **Chuan-ju Liu**[a,e,¶]

[a]Department of Orthopaedic Surgery, New York University Medical Center, New York, NY, 10003, USA

[b]Department of Orthopaedic Surgery, Jinan Central Hospital, Cheeloo College of Medicine, Shandong University, Jinan, Shandong, 250013, China

[c]Department of Orthopaedic Surgery, Qilu Hospital, Cheeloo College of Medicine, Shandong University, Jinan, Shandong, 250012, China

[d]College of Dentistry, New York University, New York, NY 10016, USA

[e]Department of Cell Biology, New York University School of Medicine, New York, NY 10016, USA

[#] These authors contributed equally to this work.

Abstract

Objectives: Type 2 diabetes mellitus (T2DM) significantly increases bone fragility and fracture risk. Progranulin (PGRN) promotes bone fracture healing in both physiological and type 1 diabetic conditions. The present study aimed to investigate the role of PGRN in T2DM bone fracture healing.

Methods: MKR (with FVB genetic background) mice were used as T2DM model. Drill-hole and Bonnarens and Einhorn models were established to investigate the role of PGRN in T2DM fracture healing *in vivo*. Primary bone marrow cells were isolated for molecular and signaling studies, and reverse transcriptase-polymerase chain reaction, immunohistochemical staining, and western blotting were performed to assess PGRN effects *in vitro*.

Results: PGRN mRNA and protein expression were upregulated in T2DM. Local administration of recombinant PGRN effectively promoted T2DM bone fracture healing *in vivo*. Additionally, PGRN could induce anabolic metabolism during endochondral ossification through TNFR2-Akt and Erk1/2 pathways. Furthermore, PGRN showed anti-inflammatory activity in the T2DM bone regeneration process.

[¶]Corresponding author: Chuan-ju Liu, Department of Orthopaedic Surgery, New York University School of Medicine, 301 East 17th Street, New York, NY 10003. Tel: 212-598-6103; Fax: 212-598-6096; Chuanju.Liu@nyulangone.org.

Author's contributions

C.L. and T.E. designed the experiments; Y.D., J.W.,and G.L. acquired the data and performed the statistical analyses; G.L. analyzed and interpreted the data; A.H. maintained the mice; J.W., A.H., X.L., and C.L. edited the manuscript. All authors drafted and reviewed the manuscript.

Conflicts of interest

The authors have no conflicts of interest to declare.

Conclusion: These findings suggest that local administration of exogenous PGRN may represent an alternative strategy to support bone regeneration in patients with T2DM. Additionally, PGRN might also hold therapeutic potential for other TNFR-related metabolic disorders.

Keywords

impaired fracture healing; progranulin; TNFα; tumor necrosis factor receptors; type 2 diabetes

1. Introduction

Type 2 diabetes mellitus (T2DM), characterized by acquired insulin resistance, is a worldwide public health concern estimated to affect 422 million people globally[1]. Systemic elevation of key inflammatory cytokines, including tumor necrosis factor-alpha (TNFα), interleukin-1β (IL-1β) and interleukin 6 (IL-6), is a well-documented feature of T2DM development. Notably, among these molecules, master inflammatory mediator TNFα has been strongly linked to the development of insulin resistance[2–5] and anti-TNFα drugs have been retrospectively indicated to promote significant improvements in fasting blood glucose, HbA1c, and fasting plasma triglyceride values for patients with T2DM[6].

Throughout the course of T2DM, complex disease-related alterations to bone metabolism and microarchitecture, and dysregulation of immune responses promote the development of concomitant bone and joint disorders, including osteomyelitis[2], increased bone fracture risk and decreased healing rates[4, 5]. Upregulation of TNFα during bone fracture healing in diabetes has been well-demonstrated by microarray and gene set enrichment analyses[7–9] and is believed to contribute to significantly delayed bone fracture healing by reducing chondrogenesis in the collagenous callus phase and by promoting osteoclastogenesis in the endochondral bone formation phase of fracture healing[10, 11]. Furthermore, both TNFα-tumor necrosis factor receptor (TNFR) signaling pathways, the proinflammatory TNFR1 and anti-inflammatory TNFR2, are known to be involved in the bone fracture healing process[12, 13]. Thus, it may be of great interest to develop novel therapies targeting TNFα/TNFRs signaling in bone regeneration for treating patients with T2DM.

Progranulin (PGRN) is a molecule with a unique beads-on-string structure, consisting of seven and a half repeats of granulin units[14–19]. Importantly, unbiased screening revealed PGRN as a TNFR binding partner capable of inhibiting TNFα:TNFR1-induced inflammation and activating anabolic TNFR2 signaling in several disease models[14, 20–23]. PGRN has been demonstrated to participate in physiological bone fracture healing primarily through promoting chondrogenesis via TNFR2 signaling[13]. Interestingly, in the type 1 diabetic bone fracture healing process, PGRN exhibits an ameliorative effect on delayed fracture healing that depends on interaction with both TNF receptors; PGRN partially accelerates callus formation through interaction with TNFR2 and partially reduces TNFα-mediated catabolism through TNFR1[12]. However, the role of PGRN in bone regeneration in T2DM remains unclear. The present study was designed to determine the role and underlying molecular mechanism of PGRN in T2DM fracture healing.

2. Materials and Methods

2.1 Media, regents, and animal models

Dulbecco′s Modified Eagle Medium (DMEM) (catalog#11965-118) was obtained from Gibco-BRL (Waltham, MA, USA). The following specific antibodies were used: anti-NOS-2 (catalog#sc-649), lamin B (catalog#sc-6217), PGNR (catalot#sc-28928) and anti-GAPDH (catalog#25778) from Santa Cruz Biotechnology (Dallas, TX, USA); anti-P38 (catalog#9212S), anti-p-P38 (catalog#9211L), anti-JNK (catalog#9258S), anti-p-JNK (catalog#4668S), and anti-P65 (catalog#8242S) from Cell Signaling Technology (Danvers, MA, USA); and anti-TNFR1 (catalog#TR76-54) and anti-TNFR2 (catalog#55R-170) from Abcam (Cambridge, UK). PathScan Multiplex Western Cocktail I (catalog#5301, an antibody cocktail, was purchased from Cell Signaling.

The collagen sponge was kindly provided by Dr. Gino Bradica (Kensey Nash Corp. Exton, PA, USA). Recombinant PGRN purification was performed as previously described[24, 25].

MKR mice have FVB/N genetic background and were obtained from Jackson Laboratory (Stock No: 016618). Both homozygous MKR mice and wildtype FVB/N mice were kept at the Skirball Institute of Biomolecular Medicine in a pathogen free environment and were housed in a 12 h light/dark cycle. Peripheral blood was drawn and glucose levels were monitored once a week. At 8 weeks of age, blood glucose levels of MKR and FVB mice were approximately 350 and 150 mg/dL, respectively. MKR mice spontaneously developed T2DM and this condition was sustained throughout the whole study, whereas FVB mice remained normoglycemic. All experiments were performed with 12 week-old male mice and were conducted in accordance with the institutional guidelines and approval from the Institutional Animal Care and Use Committee of the New York University.

2.2 Bonnarens and Einhorn bone fracture model

A closed fracture was established using the Bonnarens and Einhorn model adapted for mice as previously described[12, 22, 26]. Briefly, a surgical plane of anesthesia was induced intraperitoneal injection of ketamine/xylazine solution (0.1 mg/kg of body weight). The right hind leg was shaved and sterilized and the mouse was placed into a supine position. Under a surgical microscope, a 0.5 centimeter longitudinal incision was made medial to the patella, the patella was laterally dislocated to expose the joint space and distal femur. A 27G needle was longitudinally inserted into the patellofemoral groove to pass through the medullary canal and the exposed advancing end was clipped and buried beneath the femoral condyles. A collagen sponge carrying PGRN (6 μg) or phosphate buffered saline (PBS) was implanted into the prospective fracture area. The incision was closed and the mice were placed supine on the support stage of the Einhorn Fracture apparatus to create a facture by an established load force induced injury. An X-ray radiograph was performed to confirm the successful generation of a closed fracture. The mice were randomly divided into three groups (n = 6 per group at each time point). Mice were euthanized and tissues were collected for histological and biochemical analysis at 10, 16, and 22 days post-surgery.

2.3 The femoral drill-hole model

A femoral drill-hole model was performed as previously described[27]. In detail, mice were anesthetized with an intraperitoneal injection of ketamine/xylazine solution (0.1 mg/kg of body weight), the right hind limb was shaved and sterilized. A 0.3 cm longitudinal incision was made on the ventral aspect of the femur under aseptic conditions. The bone was exposed and an 0.8 mm diameter electronic drill was used to create a unicortical hole. The wound was irrigated with sterile saline solution and a collagen sponge containing PGRN (6 μg) or PBS was placed into the defect. The muscle, joint and skin were closed with layered sutures. Each treatment group comprised of six mice, which were euthanized for tissue harvest 10 days after the surgery.

2.4 Micro-computed tomography (CT) analysis

Micro-CT analysis was performed as previously described[28]. Briefly, tissues were harvested and fixed in 4% paraformaldehyde at room temperature for one day. Afterwards, the tissues were thrice washed with PBS and stored in 70% alcohol for micro-CT processing. Skyscan 1172 cone-beam scanner (Skyscan 1172) was used for tissue scanning. X-ray tube potential, X-ray intensity, and voxel size were set at 55 kVp, 145 mA, and 10.5 μm^3 respectively. The femoral long bone was scanned in entirety and reconstructed transaxial datasets were used for assessment of morphometric parameters of bone quality. Each sample was manually segmented to generate a region of interest excluding cortical bone; segmentation was performed over 200 slices for each sample.

2.5 Isolation of Bone marrow-cells and callus tissue

Bone marrow cells were collected from tibias following sacrifice. Tibias were excised and the two ends of the bone were cut. The bone placed into an Eppendorf tube with 100 μL of DMEM, and centrifuged at 3,000 rpm for 3 minutes to spin down bone marrow cells. The pelleted cells were resuspended with complete medium and seeded for further experiments.

The mice of Bonnarens and Einhorn bone fracture model were sacrificed on days 10, 16 and 22 post surgery. Femurs will be harvested and the soft tissue will be carefully removed. The fracture callus and 1 mm of normal bone margin was carefully excised using a scalpel. These samples were frozen in liquid N2, pulverized using a nitrogen-cooled mortar and pestle apparatus (Bel-Art, Scienceware, Pequannock, NJ, USA) and these samples were collected for extraction of mRNA and protein.

2.6 Real-time reverse transcriptase-polymerase chain reaction (RT-PCR)

Primary callus and bone marrow cells were collected for examination of transcriptional expression patterns[29]. RNeasy kit (Qiagen, Hilden, Germany) and the ImProm-II™ Reverse Transcription System (Promega Corporation Madison, WI, USA) were used for RNA extraction and cDNA synthesis in accordance with the manufacturers' instructions. The real-time PCR reaction was conducted using the 20-μL SYBR Green system (ThermoFisher Scientific, Waltham, MA, USA) in a 96-well optical reaction plate and the 7300 Sequence Detection System (Applied Biosystems, Waltham, MA, USA). The reaction was carried out over 40 cycles at temperature of 95°C for 15 seconds and 1 minute at temperature of 60°C. Glyceraldehyde 3-phosphate dehydrogenase (GAPDH) was employed

as an internal control of RNA quality. Primer was designed by Takara Biotechnology Co., Ltd., Tokyo, Japan. Each analysis was repeated in three independent experiments. The specific primer sequences are indicated in Table 1.

2.7 Western blotting

Primary callus and primary bone marrow cells were harvested in with RIPA lysis buffer with protease inhibitors (Santa Cruz Biotechnology, Inc., Dallas, TX, USA) for blotting analysis as described previously[12]. Total protein samples were loaded onto 10% sodium dodecyl sulfate-polyacrylamide gels, and were electro-transferred onto a nitrocellulose membrane at 100V over 60 min. Following membrane blockage with 5% fat-reduced milk at 25 °C for 1 hour, the membrane was washed thrice with gentle agitation in TBST at 25 °C for 10 min each time. The membrane was incubated with specific primary antibodies (1:1,000 dilution) overnight at 4 °C with agitation. After three additional washes, the membrane was incubated with horseradish peroxidase-conjugated anti-mouse secondary antibody (1:3,000 dilution; Jackson Immunology Research, West Grove, PA, USA) for 1 hour at 25 °C on an orbital shaker. The membrane was washed thrice more and the targeted proteins were visualized using an enhanced chemiluminescence system (Amersham Life Science, Little Chalfont, UK).

2.8 Histology

Femurs were fixed in 4% paraformaldehyde at room temperature. After 24 h, the samples were washed thrice with PBS, and were decalcified by 10% EDTA solution over the course of 2 weeks at 4°C. Decalcified tissues were embedded into paraffin blocks and cut into 5 μm-thick serial tissue sections. The tissue sections were stained with Safranin-O/fast green or hematoxylin-eosin (HE) using standard protocols[30, 31]. Immunohistochemistry was performed as follows. Sections were deparaffinized by xylene immersion, rehydrated by graded ethanol, and treated with 0.1% trypsin for 30 minutes at 37°C. After blocking in 20% goat serum for 60 minutes at room temperature, these sections were incubated with anti-PGRN polyclonal antibody (1:100 dilution; Santa Cruz Biotechnology) and anti-Col II (1:50 dilution; Abcam) polyclonal antibody at 4°C overnight, followed by incubation with a horseradish peroxidase–conjugated secondary antibody for 60 minutes at room temperature. The signal of PGRN and Col II was detected using the Vector Elite ABC Kit (Vectastain; Vector).

2.9 Immunofluorescence staining

Primary bone marrow cells were isolated form MKR mice and seeded on glass coverslips. The cells were incubated in the absence or presence of TNFα (10 ng/mL) in combination with or without PGRN (200 ng/mL) at 4 °C overnight. Following treatment, the medium was removed and cells were fixed using cold acetone/methanol (1:1). Cells were air-dried and rehydrated following fixation. The samples were blocked with 50% goat serum for 30 min at room temperature, and incubated with primary antibody against p65 (1:50 dilution) for 1 h at room temperature. After washing, a secondary goat anti-rabbit IgG antibody conjugated with fluorescein isothiocyanate (Santa Cruz Biotechnology #SC-2012) diluted 1:100 was added for 1 hour at room temperature, and 4,6-diamidino-2-phenylindole (DAPI) was used for

staining nuclei. Image software (Media Cybernetics, Rockville, MD, USA) was used to the capture images under Zeiss Axioscope A1 microscope.

2.10 Statistical analysis

The SPSS Statistics for Windows version 17.0 (SPSS Inc, Chicago, IL, USA) was used for standard statistical analyses, including one-way analysis of variance (ANOVA) and Student's *t*-test. Statistical significance was achieved at $p < 0.05$.

3. Results

3.1 PGRN expression is upregulated in T2DM

Bone marrow cells isolated from FVB control and MKR diabetic mice were evaluated to investigate whether PGRN expression was altered under T2DM condition. At the age of 12 weeks, the transcriptional level of *GRN* was found to be significantly increased in MKR mice compared with their control littermates (Fig. 1A). This change was accompanied by a marked increase in PGRN protein levels, as detected by western blotting (Fig. 1B). Next, we examined PGRN expression at the mRNA and protein levels during the diabetic fracture healing process. Calluses were harvested from MKR and FVB mice at day 10, 16 and 22 post-induction of the closed *Bonnarens and Einhorn* fracture model and processed for RT-PCR or western blotting. Transcriptional and protein levels of PGRN were strongly increased under T2DM condition (Fig. 1C, D). Additionally, immunohistochemical staining of cartilaginous callus tissues collected at day 10 post-operation revealed that PGRN expression was dramatically upregulated in the impaired bone fracture healing process in MKR mice relative to levels expressed under physiological conditions in FVB mice (Fig. 1E).

3.2 PGRN promotes bone fracture healing in drill-hole murine model with T2DM

A murine femoral drill-hole model was established and recombinant PGRN was locally administered. The femur was collected for analysis 10 days post-surgery. Micro-CT images revealed the formation of the callus under normoglycemic conditions in FVB mice (Fig. 2A). In contrast, almost no callus was formed under hyperglycemia in MKR mice. Interestingly, addition of recombinant PGRN effectively promoted callus formation under T2DM condition (Fig. 2A). Furthermore, bone volume fraction (BV/TV) was significantly reduced in the T2DM bone healing process compared with physiological conditions (Fig. 2B). However, local administration of recombinant PGRN was associated with increased BV/TV in T2DM, reaching levels comparable to non-T2DM mice. Further tissue analysis by HE staining also suggested reduced callus formation in the MKR group compared with FVB mice (Fig. 2C), which was improved following introduction of recombinant PGRN.

3.3 PGRN promotes T2DM-delayed bone regeneration in Bonnarens and Einhorn fracture mouse model

To further confirm the role of PGRN in the type 2 diabetic fracture healing, femoral tissues were harvested on days 10, 16, and 22 post-induction of a murine *Bonnarens and Einhorn* fracture model. The callus was largely formed by day 10, new bone formation was identified on day 16, and the bone was almost healed in the FVB control group and MKR-PGRN-

treated mice by day 22 (Fig. 3A). However, in the MKR-PBS-treated group, less callus was formed at days 10 and 16 relative to other treatment groups. Importantly, callus and persistent bone non-union was observed through day 22 in the MKR-PBS-treated mice. The proportion of cartilage and bone in the callus area was quantified based on the histological staining. As suggested in Fig. 3B–D, MKR-PBS-treated mice exhibited significantly reduced cartilage area and proportion, as well as bone formation proportion, compared with FVB-PBS-treated and MKR-PGRN-treated mice at each time point.

3.4 PGRN promotes chondrogenesis in T2DM

To investigate the role of PGRN in callus transformation throughout diabetic bone fracture healing, callus tissues were collected on day 10 post-surgery and evaluated by immunohistochemical staining and rtPCR analysis of chondrogenic markers. Type 2 collagen (Col II) expression in MKR-PBS-treated group was dramatically reduced compared with FVB-PBS-treated and MKR-PGRN-treated mice (Fig. 4A), which exhibited comparable Col II expression. Moreover, the transcriptional levels of *COL2A1* and *ACAN*, which encode the chondrogenesis biomarkers Col II and aggrecan, were found to be significantly higher in FVB-PBS-treated and MKR-PGRN-treated groups than in MKR-PBS-treated mice on days 10 and 16 (Fig. 4B,C). Importantly, transcriptional data suggested that Col II and *ACAN* expression gradually decreased during the bone healing process.

PGRN has demonstrated to be an inducer of chondrocyte differentiation under physiological and type 1 diabetic conditions. Therefore, we examined whether PGRN maintained such activity in T2DM. Isolated bone marrow cells from MKR and FVB mice were incubated with or without recombinant PGRN for 8 hours. The presence of PGRN was associated with significant increase in the transcriptional levels of *COL2A1* and *ACAN* under both physiological and T2DM conditions (Fig. 4D,E). Notably, PGRN-induced *COL2A1* and *ACAN* expression was significantly reduced with T2DM compared with the normoglycemic condition.

3.5 PGRN suppresses TNFα-induced inflammation in T2DM mice

Given the demonstrated potential of recombinant PGRN in restoration of bone fracture healing in T2DM mice, additional experiments were performed to shed light onto the molecular mechanisms involved in this process. PGRN is known to inhibit TNFα-induced catabolism under both physiological and type 1 diabetic circumstances[12] and to be upregulated in T2DM. Real-time PCR assay with primary bone marrow cells from control FVB and diabetic MKR mice indicated that TNFR1 was increased, whereas the level of TNFR2 was not significantly changed in MKR mice (data not shown). Therefore, it was first determined whether PGRN blocked T2DM-induced inflammation. Analysis of callus collected following *Bonnarens and Einhorn* fracture revealed that the expressions of pro-inflammatory cytokines, including IL-1β, COX-2, and NOS-2, were significantly higher in the MKR-PBS-treated group than in FVB-PBS-treated and MKR-PGRN-treated groups (Fig. 5A–C). NOS-2, which is a well-accepted severity marker of inflammation, was found to be increased in T2DM animals (Fig. 5D). However, this pro-inflammatory signal was significantly inhibited in the presence of recombinant PGRN.

To further examine the involved molecular events, isolated primary bone marrow cells were incubated with or without TNFα and in absence or presence of recombinant PGRN. Western blot analysis showed that JNK and P38 were activated under normoglycemic condition in the presence of TNFα, and were further enhanced in cells isolated from T2DM mice (Fig. 5E). Interestingly, addition of PGRN inhibited the activation of these pathways. However, the phosphorylation levels of JNK and P38 were still higher in T2DM in the presence of PGRN than in physiological conditions.

NF-κB signaling is a classic pathway that can be activated by TNFα. After activation, p65 is phosphorylated and translocated into the cell nuclei, which will in turn promote the transcription of downstream targeted genes. To determine the role of PGRN in the NF-κB pathway, bone marrow cells were treated as mentioned above, and nuclear and cytoplasmic proteins were extracted separately. Analysis of p65 revealed that it was translocated from the cytoplasm to the nuclei upon TNFα treatment in both control and T2DM groups, and that this translocation could be inhibited by PGRN (Fig. 5F). Immunostaining further confirmed that TNFα enhanced p65 translocation, while addition of PGRN effectively inhibited p65 translocation in T2DM (Fig. 5G). Consequently, the transcriptional levels of downstream inflammatory molecules, including IL-1β, COX-2 and NOS-2, were significantly reduced by PGRN in both physiological and diabetic conditions (Fig. 5H–J). Western blot data also confirmed these findings, as shown in Fig. 5K. PGRN inhibited TNFα-mediated NOS-2 expression.

3.6 PGRN accelerates bone fracture healing via TNFR2-Akt and Erk1/2 signaling in T2DM

The therapeutic and protective capacity of PGRN is mainly achieved through TNFR2-mediated signaling in many TNFR-related diseases, including inflammatory and degenerative arthritis[23, 25, 32]. Therefore, the involvement of the TNFR2 pathway in PGRN-promoted bone fracture healing in T2DM was also evaluated. Isolated bone marrow cells were cultured in the absence or presence of PGRN, as well as with TNFR1 or TNFR2 blocking antibodies (final concentration of 1 μg/mL). PGRN was found to significantly increase the levels of chondrogenic anabolic biomarkers in T2DM (Fig. 6A,B), with *COL2A1* and *ACAN* expression being partially impaired when TNFR1 was blocked. Importantly, the anabolic effect of PGRN was abrogated when TNFR2 was blocked. Additional analysis of primary bone marrow cells from FVB and MKR mice also showed that PGRN strongly activated Akt and Erk1/2 signaling in both normal and diabetic conditions (Fig. 6C). Notably, PGRN-mediated Akt and Erk1/2 activation was slightly reduced in MKR compared with FVB mice. Additionally, the effects of PGRN on Akt and Erk1/2 activation remained unaltered in the presence of a TNFR1-blocking antibody, whereas it was lost when TNFR2 was blocked (Fig. 6D). Collectively, PGRN was found to effectively promote the anabolic metabolism through TNFR2, Akt, and Erk1/2 pathways in T2DM.

4. Discussion

Diabetes mellitus is a global health concern projected to affect up to 629 million people over the next 25 years[33]. Patients with diabetes clinically exhibit prolonged bone fracture

healing process, or even bone nonunion, which can be accompanied by unrepaired wound site due to diabetes-related or diabetes-induced immune inflammatory environment[34]. The limiting step of the bone fracture healing process is the formation of collagenous callus and endochondral ossification of the callus. Large scale unbiased screening has demonstrated that TNFα expression is dramatically increased in the callus stage in the process of bone healing and that it effectively induces chondrocyte apoptosis, which largely delays the transition of callus to bone ossification[11, 35]. Interestingly, administration of anti-TNFα drugs to diabetic mice has been shown to generate significant reduction in chondrocyte apoptosis in comparison with their control littermates, resulting in accelerated bone regeneration in the diabetic setting[8]. Notably, TNFα is also believed to be a critical molecule for insulin resistance in diabetes[36], with studies suggesting that anti-TNFα treatments can prevent insulin resistance[6]. Taken together, targeting TNFα signaling may be a potential avenue for treating diabetic bone fractures.

PGRN is a TNFR binding partner and downstream molecule of BMP-2 capable of accelerating physiological and T1DM fracture healing through activating TNFR2 mediated chondrogenic signaling and modulating TNFα:TNFR1 induced catabolism[12, 13, 24, 37–40]. Here we examined the role of PGRN in fracture healing in the T2DM microenvironment. In agreement with reports of elevated PGRN levels in sera of patients with T2DM compared with healthy people[41], the present study showed that PGRN expression was significantly upregulated in bone marrow cells, as well as in the bone fracture site of T2DM model mice. Similar to the T1DM condition, local administration of PGRN promoted the fracture healing process in T2DM mice. Specifically, PGRN reduced TNFR1-mediated catabolism and induced TNFR2-mediated anabolism, ultimately overcoming the effects of T2DM on fracture healing rates.

People with T2DM have normal or even higher bone mineral density (BMD) compared with healthy people[42]; however, people with T2DM have markedly higher risk for fracture[43, 44]. Studies have demonstrated that the bone strength is decreased in T2DM and that the bone microarchitecture is changed, especially affecting the cortical bone, leading to increased fragility[45]. In addition, evidenced by impaired bone formation, data suggest that the bone turnover is also reduced in T2DM[46]. Indeed, the total bone mass remains the same or is even increased in T2DM, but the bone metabolism is disturbed and the bone mass is insufficient for normal biomechanical force. In the present study it was demonstrated that local PGRN administration could significantly improve local BV/TV in the T2DM fracture healing site, suggesting that PGRN can effectively promote diabetic fracture healing. However, whether and how PGRN affects the systemic bone metabolism in T2DM needs to be further investigated. Notably, changes in bone microarchitecture observed in T2DM MKR mice may be, at least in part, dependent upon muscle hypoplasia and skeletal muscle hypertrophy inherent in the MKR model.

The role of PGRN in the diabetic microenvironment is shrouded in some controversy. Some investigations have claimed that PGRN level was related to obesity-associated pathologies, including diabetes[47, 48], wherein PGRN ostensibly acts as a pro-inflammatory cytokine responsible for insulin resistance by mediating interleukin (IL)-6 production[49, 50]. Conversely, additional studies have reported little relation between PGRN and insulin

resistance[51, 52]. Moreover, genetic loss of PGRN was shown to induce nephrogenic diabetes insipidus in aging mice, indicating that PGRN might be protective against diabetes [53]. Notably, full-length PGRN can be cleaved to form pro-inflammatory granulin subunits, and the PGRN/granulin ratio is also believed to be a marker of inflammatory status [54]. Unfortunately, all commercially available ELISA kits measure the total levels of PGRN, and cannot distinguish the full length PGRN and its degradative subunits. In the present study, recombinant PGRN was administrated locally instead of systemically in an effort to minimize interaction between PGRN with proteinases for cleavage. Another important factor to be considered while evaluating potential inconsistencies in PGRN's role is the experimental models used; while previous studies have focused on the effects of PGRN on adipocytes[55–57], here we addressed the role of PGRN in bone marrow cell differentiation.

Despite the controversies concerning PGRN's role in T2DM, the present study demonstrated that local application of exogenous PGRN can promote bone fracture healing in T2DM. In particular, PGRN can block catabolic destruction through the TNFR1 pathway, resulting in reduced inflammation. Moreover, PGRN enhances chondrogenesis, leading to accelerated callus formation and improved endochondral ossification *in vivo*. Collectively, these findings indicate that local administration of PGRN can support fracture healing in T2DM.

Acknowledgments

This work was supported by the National Institutes of Health (research grants R01AR076900, R01AR062207, R01AR061484, and 1R01NS103931) and a U.S. Department of Defense research grant (W81XWH-16-1-0482, to C. J. Liu).

Reference

1. Compston J, Type 2 diabetes mellitus and bone. J Intern Med, 2018. 283(2): p. 140–153. [PubMed: 29265670]
2. Banks WA, et al., Insulin resistance syndrome in the elderly: assessment of functional, biochemical, metabolic, and inflammatory status. Diabetes Care, 2007. 30(9): p. 2369–73. [PubMed: 17536070]
3. Hotamisligil GS, The role of TNFalpha and TNF receptors in obesity and insulin resistance. J Intern Med, 1999. 245(6): p. 621–5. [PubMed: 10395191]
4. Schwartz SS, et al., The Time Is Right for a New Classification System for Diabetes: Rationale and Implications of the beta-Cell-Centric Classification Schema. Diabetes Care, 2016. 39(2): p. 179–86. [PubMed: 26798148]
5. Shoelson SE, Lee J, and Goldfine AB, Inflammation and insulin resistance. J Clin Invest, 2006. 116(7): p. 1793–801. [PubMed: 16823477]
6. Gupta-Ganguli M, et al., Does therapy with anti-TNF-alpha improve glucose tolerance and control in patients with type 2 diabetes? Diabetes Care, 2011. 34(7): p. e121. [PubMed: 21709287]
7. Alblowi J, et al., Chemokine expression is upregulated in chondrocytes in diabetic fracture healing. Bone, 2013. 53(1): p. 294–300. [PubMed: 23262028]
8. Lim JC, et al., TNFalpha contributes to diabetes impaired angiogenesis in fracture healing. Bone, 2017. 99: p. 26–38. [PubMed: 28285015]
9. Sun M, et al., TNF-alpha is upregulated in T2DM patients with fracture and promotes the apoptosis of osteoblast cells in vitro in the presence of high glucose. Cytokine, 2016. 80: p. 35–42. [PubMed: 26945994]
10. Kayal RA, et al., Diabetes causes the accelerated loss of cartilage during fracture repair which is reversed by insulin treatment. Bone, 2009. 44(2): p. 357–63. [PubMed: 19010456]

11. Kayal RA, et al., TNF-alpha mediates diabetes-enhanced chondrocyte apoptosis during fracture healing and stimulates chondrocyte apoptosis through FOXO1. J Bone Miner Res, 2010. 25(7): p. 1604–15. [PubMed: 20200974]
12. Wei J, et al., Progranulin promotes diabetic fracture healing in mice with type 1 diabetes. Ann N Y Acad Sci, 2020. 1460(1): p. 43–56. [PubMed: 31423598]
13. Zhao YP, et al., The promotion of bone healing by progranulin, a downstream molecule of BMP-2, through interacting with TNF/TNFR signaling. Biomaterials, 2013. 34(27): p. 6412–21. [PubMed: 23746860]
14. Jian J, Konopka J, and Liu C, Insights into the role of progranulin in immunity, infection, and inflammation. J Leukoc Biol, 2013. 93(2): p. 199–208. [PubMed: 23089745]
15. Jian J, et al., Progranulin: A key player in autoimmune diseases. Cytokine, 2018. 101: p. 48–55. [PubMed: 27527809]
16. Liu CJ, Progranulin: a promising therapeutic target for rheumatoid arthritis. FEBS Lett, 2011. 585(23): p. 3675–80. [PubMed: 21550343]
17. Liu CJ and Bosch X, Progranulin: A growth factor, a novel TNFR ligand and a drug target. Pharmacol Ther, 2012. 133(1): p. 124–32. [PubMed: 22008260]
18. Wei J, Hettinghouse A, and Liu C, The role of progranulin in arthritis. Ann N Y Acad Sci, 2016. 1383(1): p. 5–20. [PubMed: 27505256]
19. Williams A, et al., Review: Novel Insights Into Tumor Necrosis Factor Receptor, Death Receptor 3, and Progranulin Pathways in Arthritis and Bone Remodeling. Arthritis Rheumatol, 2016. 68(12): p. 2845–2856. [PubMed: 27428882]
20. Cui Y, Hettinghouse A, and Liu CJ, Progranulin: A conductor of receptors orchestra, a chaperone of lysosomal enzymes and a therapeutic target for multiple diseases. Cytokine Growth Factor Rev, 2019. 45: p. 53–64. [PubMed: 30733059]
21. Ding H, et al., Progranulin derived engineered protein Atsttrin suppresses TNF-alpha-mediated inflammation in intervertebral disc degenerative disease. Oncotarget, 2017. 8(65): p. 109692–109702. [PubMed: 29312639]
22. Kayal RA, et al., Diminished bone formation during diabetic fracture healing is related to the premature resorption of cartilage associated with increased osteoclast activity. J Bone Miner Res, 2007. 22(4): p. 560–8. [PubMed: 17243865]
23. Wei JL, et al., Role of ADAMTS-12 in Protecting Against Inflammatory Arthritis in Mice By Interacting With and Inactivating Proinflammatory Connective Tissue Growth Factor. Arthritis Rheumatol, 2018. 70(11): p. 1745–1756. [PubMed: 29750395]
24. Feng JQ, et al., Granulin epithelin precursor: a bone morphogenic protein 2-inducible growth factor that activates Erk1/2 signaling and JunB transcription factor in chondrogenesis. FASEB J, 2010. 24(6): p. 1879–92. [PubMed: 20124436]
25. Tang W, et al., The Growth Factor Progranulin Binds to TNF Receptors and Is Therapeutic Against Inflammatory Arthritis in Mice. Science, 2011. 332(6028): p. 478–484. [PubMed: 21393509]
26. Ko KI, et al., Diabetes reduces mesenchymal stem cells in fracture healing through a TNFalpha-mediated mechanism. Diabetologia, 2015. 58(3): p. 633–642. [PubMed: 25563724]
27. Zhao YP, et al., The promotion of bone healing by progranulin, a downstream molecule of BMP-2, through interacting with TNF/TNFR signaling. 2013. 34(27): p. 6412–6421.
28. Progranulin promotes diabetic fracture healing in mice with type 1 diabetes %J Annals of the New York Academy of ences. 2020. 1460(1).
29. Wei JL, et al., Role of ADAMTS-12 in Protecting Against Inflammatory Arthritis in Mice By Interacting With and Inactivating Proinflammatory Connective Tissue Growth Factor. 2018. 70(11).
30. Fu W, et al., Foxo4- and Stat3-dependent IL-10 production by progranulin in regulatory T cells restrains inflammatory arthritis. FASEB J, 2017. 31(4): p. 1354–1367. [PubMed: 28011648]
31. Lai Y, et al., ADAMTS-7 forms a positive feedback loop with TNF-alpha in the pathogenesis of osteoarthritis. Ann Rheum Dis, 2014. 73(8): p. 1575–84. [PubMed: 23928557]
32. Zhao YP, et al., Progranulin protects against osteoarthritis through interacting with TNF-alpha and beta-Catenin signalling. Ann Rheum Dis, 2015. 74(12): p. 2244–53. [PubMed: 25169730]

33. Lim RR, et al., NOD-like Receptors in the Eye: Uncovering Its Role in Diabetic Retinopathy. Int J Mol Sci, 2020. 21(3).
34. Hunt HB, et al., Altered Tissue Composition, Microarchitecture, and Mechanical Performance in Cancellous Bone From Men With Type 2 Diabetes Mellitus. J Bone Miner Res, 2019. 34(7): p. 1191–1206. [PubMed: 30866111]
35. Alblowi J, et al., High levels of tumor necrosis factor-alpha contribute to accelerated loss of cartilage in diabetic fracture healing. Am J Pathol, 2009. 175(4): p. 1574–85. [PubMed: 19745063]
36. Mohamad HE, et al., Infliximab ameliorates tumor necrosis factor-alpha exacerbated renal insulin resistance induced in rats by regulating insulin signaling pathway. Eur J Pharmacol, 2020. 872: p. 172959. [PubMed: 32004528]
37. Alquezar C, et al., Progranulin deficiency induces overactivation of WNT5A expression via TNF-alpha/NF-kappaB pathway in peripheral cells from frontotemporal dementia-linked granulin mutation carriers. J Psychiatry Neurosci, 2016. 41(4): p. 225–39. [PubMed: 26624524]
38. Pearson-Stuttard J, et al., Diabetes and infection: assessing the association with glycaemic control in population-based studies. Lancet Diabetes Endocrinol, 2016. 4(2): p. 148–58. [PubMed: 26656292]
39. Wang BC, et al., New discovery rarely runs smooth: an update on progranulin/TNFR interactions. Protein Cell, 2015. 6(11): p. 792–803. [PubMed: 26408020]
40. Wang S, et al., Progranulin Is Positively Associated with Intervertebral Disc Degeneration by Interaction with IL-10 and IL-17 Through TNF Pathways. Inflammation, 2018. 41(5): p. 1852–1863. [PubMed: 29992506]
41. Nguyen AD, et al., Progranulin: at the interface of neurodegenerative and metabolic diseases. Trends Endocrinol Metab, 2013. 24(12): p. 597–606. [PubMed: 24035620]
42. Lekkala S, et al., Effects of Diabetes on Bone Material Properties. Curr Osteoporos Rep, 2019. 17(6): p. 455–464. [PubMed: 31713179]
43. Acevedo C, et al., Contributions of Material Properties and Structure to Increased Bone Fragility for a Given Bone Mass in the UCD-T2DM Rat Model of Type 2 Diabetes. J Bone Miner Res, 2018. 33(6): p. 1066–1075. [PubMed: 29342321]
44. Samelson EJ, et al., Diabetes and Deficits in Cortical Bone Density, Microarchitecture, and Bone Size: Framingham HR-pQCT Study. J Bone Miner Res, 2018. 33(1): p. 54–62. [PubMed: 28929525]
45. Picke AK, et al., Update on the impact of type 2 diabetes mellitus on bone metabolism and material properties. Endocr Connect, 2019. 8(3): p. R55–R70. [PubMed: 30772871]
46. Lecka-Czernik BJSOC, Diabetes, bone and glucose-lowering agents: basic biology. 2017. 60(7).
47. Albeltagy ES, Hammour AE, and Albeltagy SA, Potential value of serum Progranulin as a biomarker for the presence and severity of micro vascular complications among Egyptian patients with type 2 diabetes mellitus. J Diabetes Metab Disord, 2019. 18(1): p. 217–228. [PubMed: 31275893]
48. Qu H, Deng H, and Hu Z, Plasma progranulin concentrations are increased in patients with type 2 diabetes and obesity and correlated with insulin resistance. Mediators Inflamm, 2013. 2013: p. 360190. [PubMed: 23476101]
49. Li H, et al., PGRN exerts inflammatory effects via SIRT1-NF-kappaB in adipose insulin resistance. J Mol Endocrinol, 2020. 64(3): p. 181–193. [PubMed: 31990656]
50. Matsubara T, et al., PGRN is a Key Adipokine Mediating High Fat Diet-Induced Insulin Resistance and Obesity through IL-6 in Adipose Tissue. Cell Metab, 2012. 15(1): p. 38–50. [PubMed: 22225875]
51. Niklowitz P, et al., Is there a link between progranulin, obesity, and parameters of the Metabolic Syndrome in children? Findings from a longitudinal intervention study. Pediatr Diabetes, 2019. 20(8): p.1047–1055 [PubMed: 31469472]
52. Fasshauer M, Blüher M, and Stumvoll MJLDE, Adipokines in gestational diabetes. Lancet Diabetes Endocrinol, 2014. 2(6): p. 488–499. [PubMed: 24731659]
53. Albeltagy ES, et al., Potential value of serum Progranulin as a biomarker for the presence and severity of micro vascular complications among Egyptian patients with type 2 diabetes mellitus. J Diabetes Metab Disord, 2019. 18(1): p. 217–228 [PubMed: 31275893]

54. Nguyen AD, et al., Progranulin: at the interface of neurodegenerative and metabolic diseases. Trends Endocrinol Metab, 2013. 24(12): p. 597–606. [PubMed: 24035620]

55. Qu H, Deng H, and Hu ZJMI, Plasma Progranulin Concentrations Are Increased in Patients with Type 2 Diabetes and Obesity and Correlated with Insulin Resistance. Mediators Inflamm, 2013. 2013(2): p. 360190.

56. Matsubara T, et al., PGRN is a Key Adipokine Mediating High Fat Diet-Induced Insulin Resistance and Obesity through IL-6 in Adipose Tissue. Cell Metab, 2012. 15(1): p. 38–50. [PubMed: 22225875]

57. Youn, et al., Serum Progranulin Concentrations May Be Associated With Macrophage Infiltration Into Omental Adipose Tissue. Diabetes, 2009. 58(3): p. 627–36 [PubMed: 19056610]

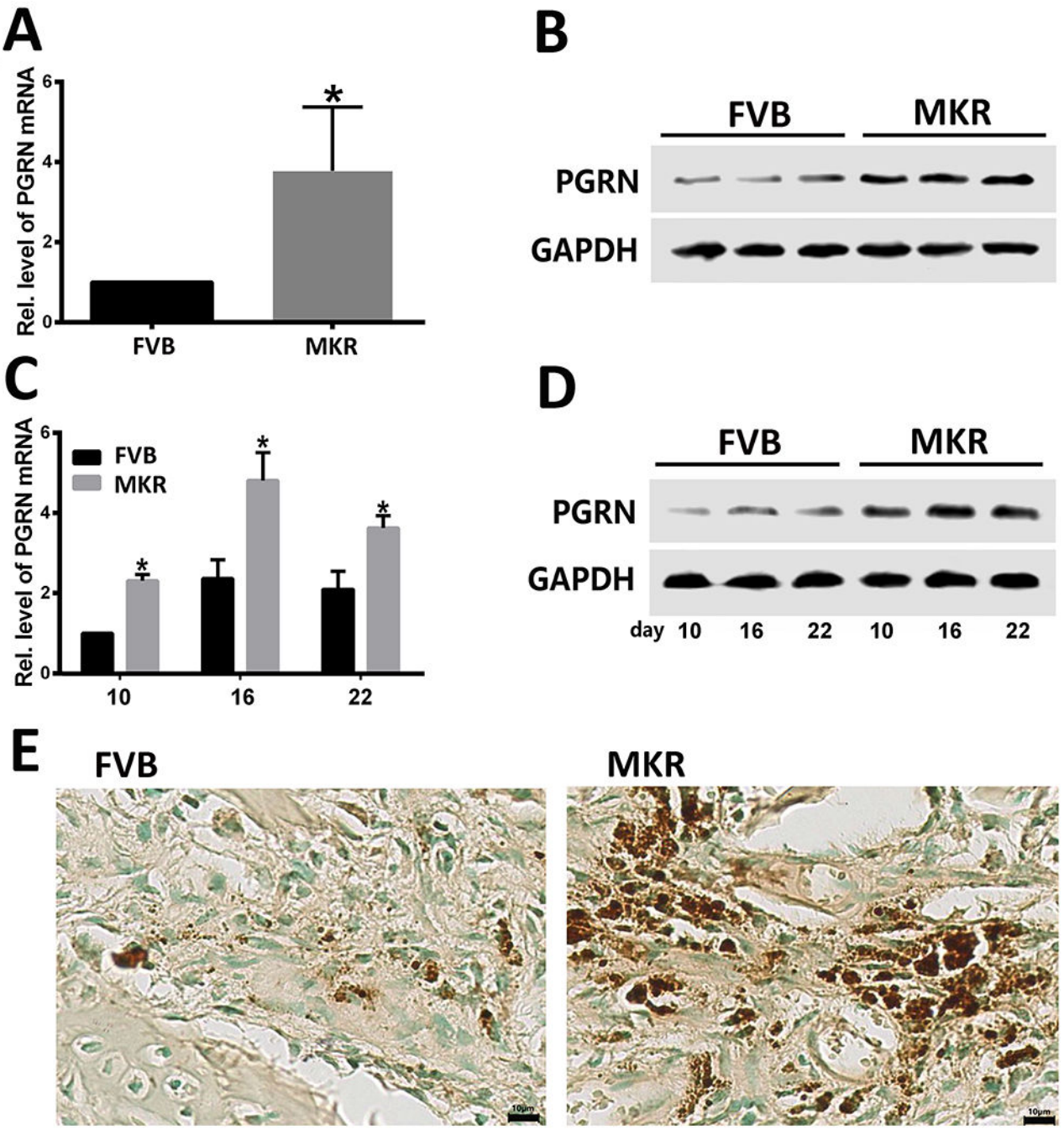

Figure.1. PGRN expression is upregulated under type 2 diabetic conditions.

(**A**) Transcriptional and (**B**) protein levels of PGRN in primary bone marrow cells as determined by reverse transcriptase-polymerase chain reaction (RT-PCR) and western blotting. (**C**) Transcriptional and (**D**) protein levels of PGRN in the callus collected from *Bonnarens and Einhorn* fractures on day 10, 16 and 22 after surgery, assessed by RT-PCR and western blotting. (**E**) Immunohistochemical (IHC) staining of PGRN. IHC positive signal is indicated in brown. *t*-test was used to assess statistical differences between groups.

The values shown represent the mean ± standard deviation of three independent experiments. *$p < 0.05$ vs. control group.

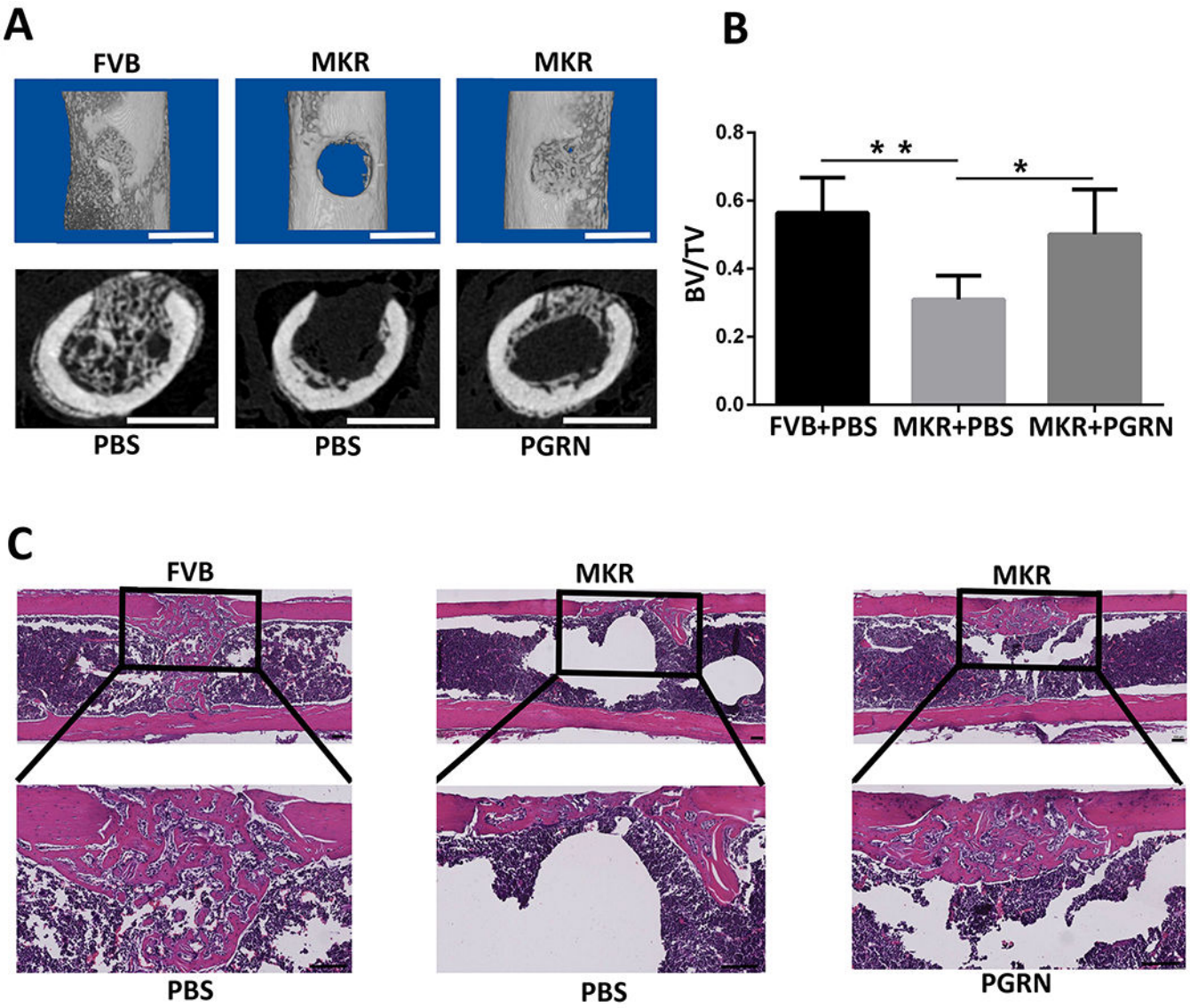

Figure.2. PGRN promotes bone fracture healing in drill-hole murine model with T2DM.

(**A**) Micro-computed tomography (CT) image of the murine femoral drill-hole model. First line: Three-dimensional reconstructed image of the femur in the drill-hole model. Second line: cross section of the micro-CT scanning. (**B**) Quantification of the bone volume fraction (BV/TV) based on the micro-CT scanning. (**C**) Hematoxylin-eosin staining of the drill-hole model. *$p < 0.05$ and ** $p < 0.01$ vs. control group.

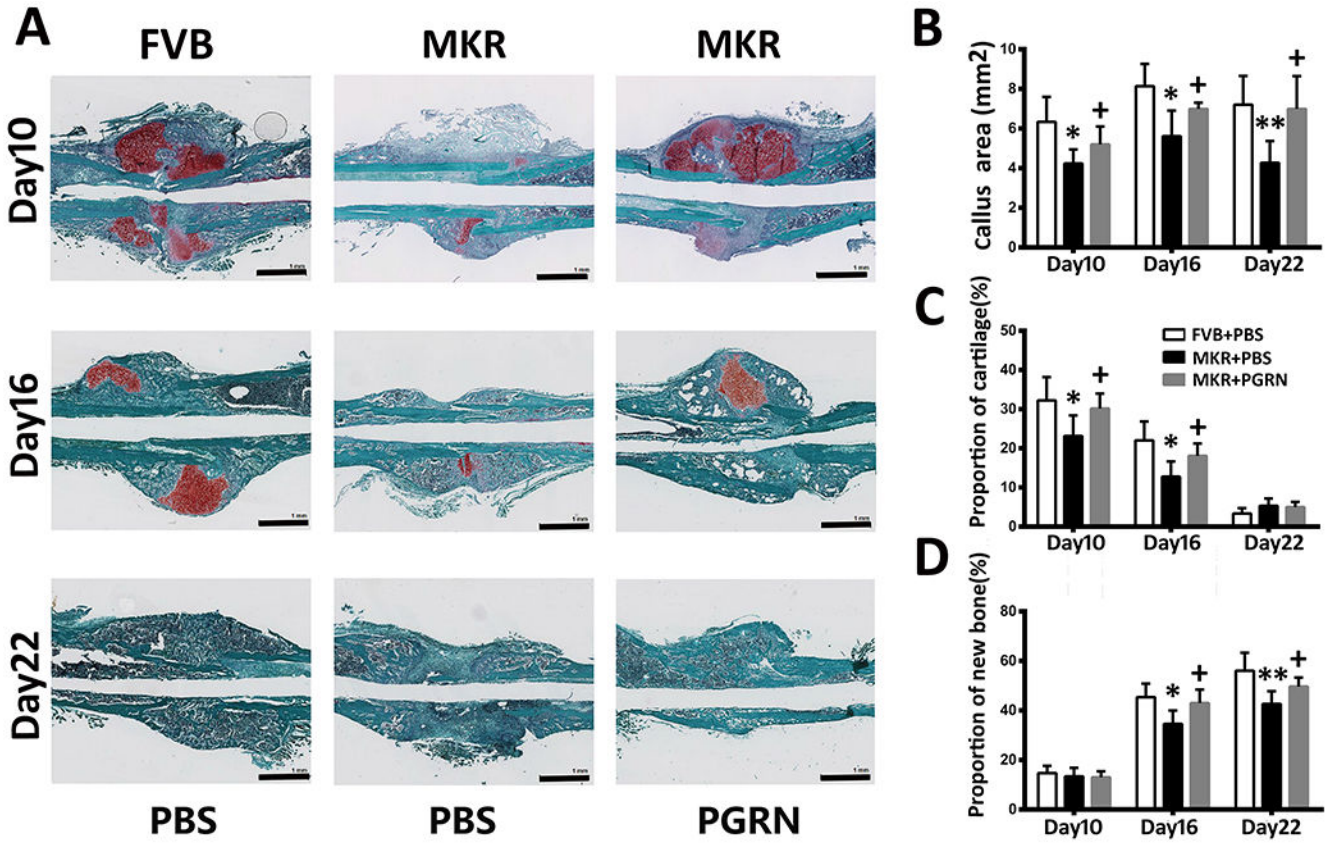

Figure.3. PGRN promotes T2DM-delayed bone regeneration in *Bonnarens and Einhorn* fracture mouse model.

(**A**) Safranin O/Fast Green staining of *Bonnarens and Einhorn* fractures at the indicated time point after surgery. (**B**) Callus area after *Bonnarens and Einhorn* fracture established at various time points based on the Safranin O/Fast Green staining. (**C**) Cartilage and (**D**) new bone formation proportion in the bone healing process based on the Safranin O/Fast Green staining. *$p < 0.05$ and ** $p < 0.01$ vs. control group.

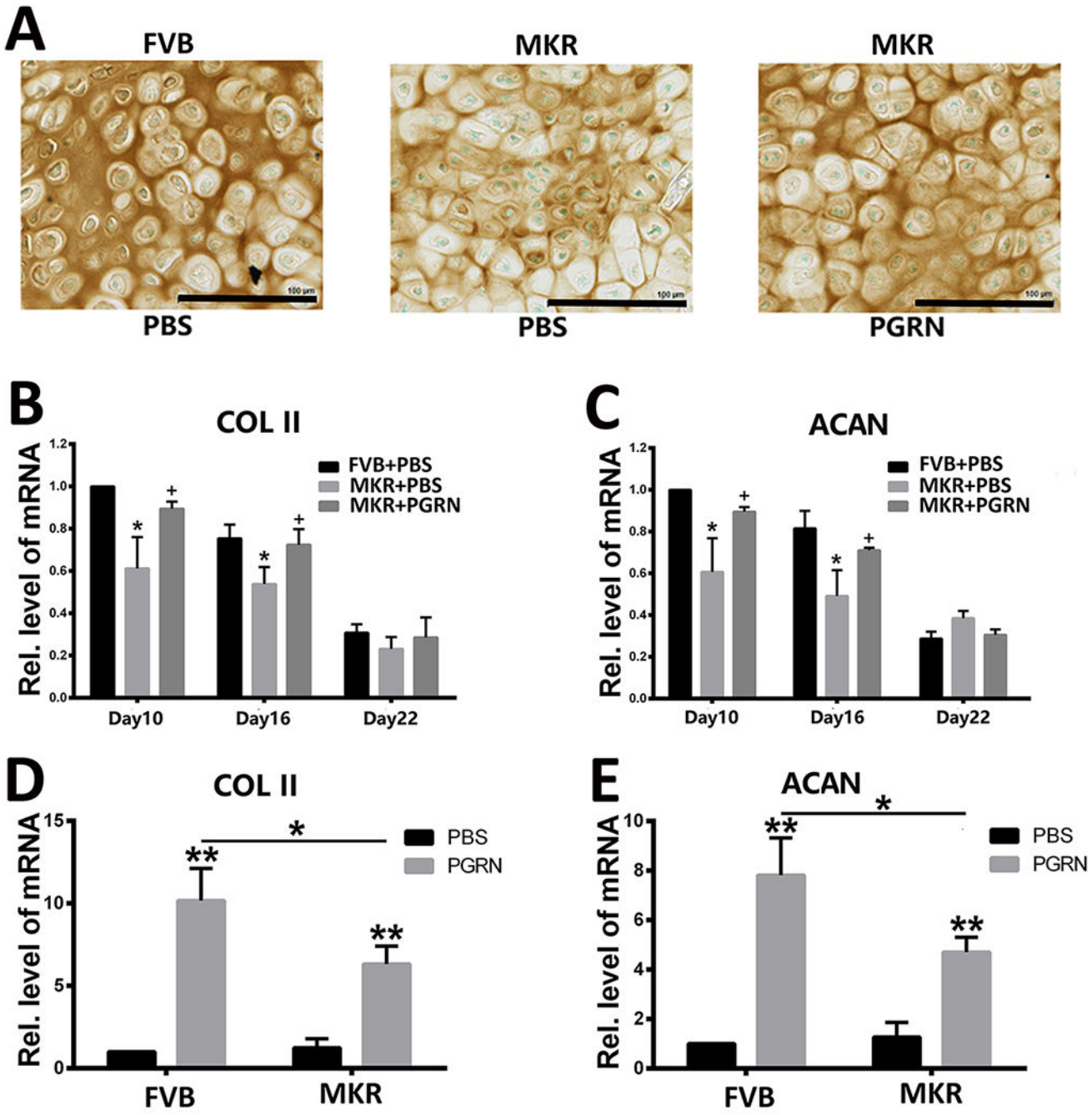

Figure.4. PGRN promotes chondrogenesis in T2DM.

(**A**) Immunohistochemical staining of type 2 collagen in the callus collected from *Bonnarens and Einhorn* fracture mice on day 10 post-surgery. Positive signal is indicated in brown. Transcriptional levels of *COL2A1* (type II collagen) and *ACAN* (aggrecan) in (**B**,**C**) the callus of *Bonnarens and Einhorn* fracture mice on day 10 post-surgery and (**D**,**E**) in primary bone marrow cells of FVB and MKR mice in absence or presence of recombinant PGRN, as determined by reverse transcriptase-polymerase chain reaction. The values shown represent

the mean ± standard deviation of three independent experiments. *$p < 0.05$ and ** $p < 0.01$ vs. control group.

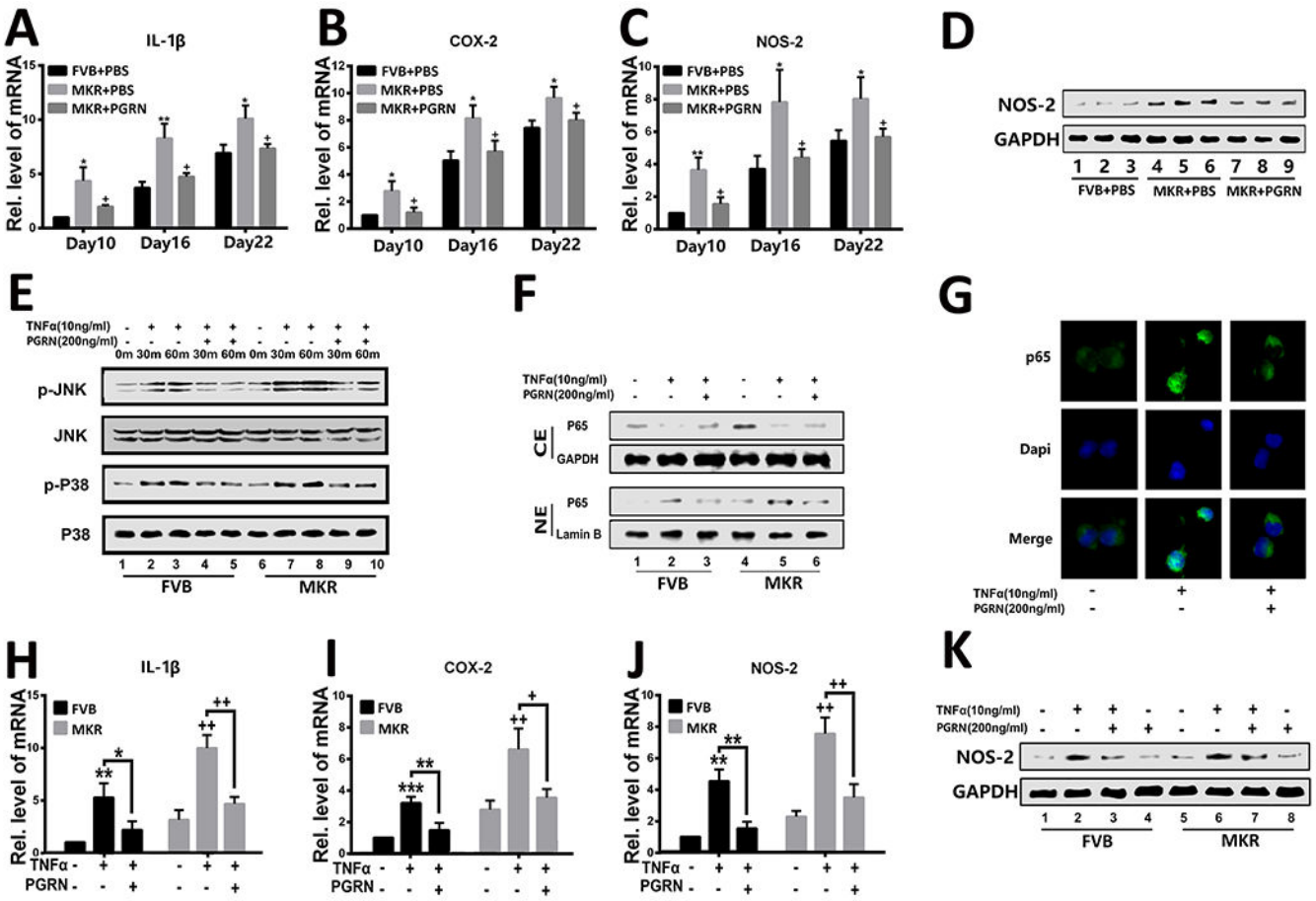

Figure.5. PGRN suppresses TNFα-induced inflammation in T2DM.

(**A–C**) Transcriptional levels of *IL1B*, *COX2*, and *NOS2* in the callus of *Bonnarens and Einhorn* fracture mice on day 10 post-surgery as determined by reverse transcriptase-polymerase chain reaction (RT-PCR). (**D**) Protein level of NOS-2 in the callus of *Bonnarens and Einhorn* fracture mice on day 10 post-surgery, as assessed by western blotting. (**E**) Activation of P38 (p-P38) and JNK (p-JNK) in primary bone marrow cells cultured without or with TNFα and/or PGRN for various time points was determined by western blotting. Total P38 and JNK served as internal controls. (**F**) P65 was determined by western blotting assay in primary bone marrow cells that were cultured with TNFα, PGRN, or both. (**G**) Immunofluorescence staining of P65 in primary bone marrow cells of MKR mice in the presence of TNFα or PGRN plus TNFα. (**H–J**) Expression of *IL1B*, *COX2*, and *NOS2* in primary bone marrow cells of FVB and MKR mice, determined by RT-PCR. (**K**) western blotting assay of NOS-2 in primary bone marrow cells cultured in the presence of TNFα, PGRN, or both for 48 hours. The values shown represent the mean ± standard deviation. *$p < 0.05$ and ** $p < 0.01$ vs. control group.

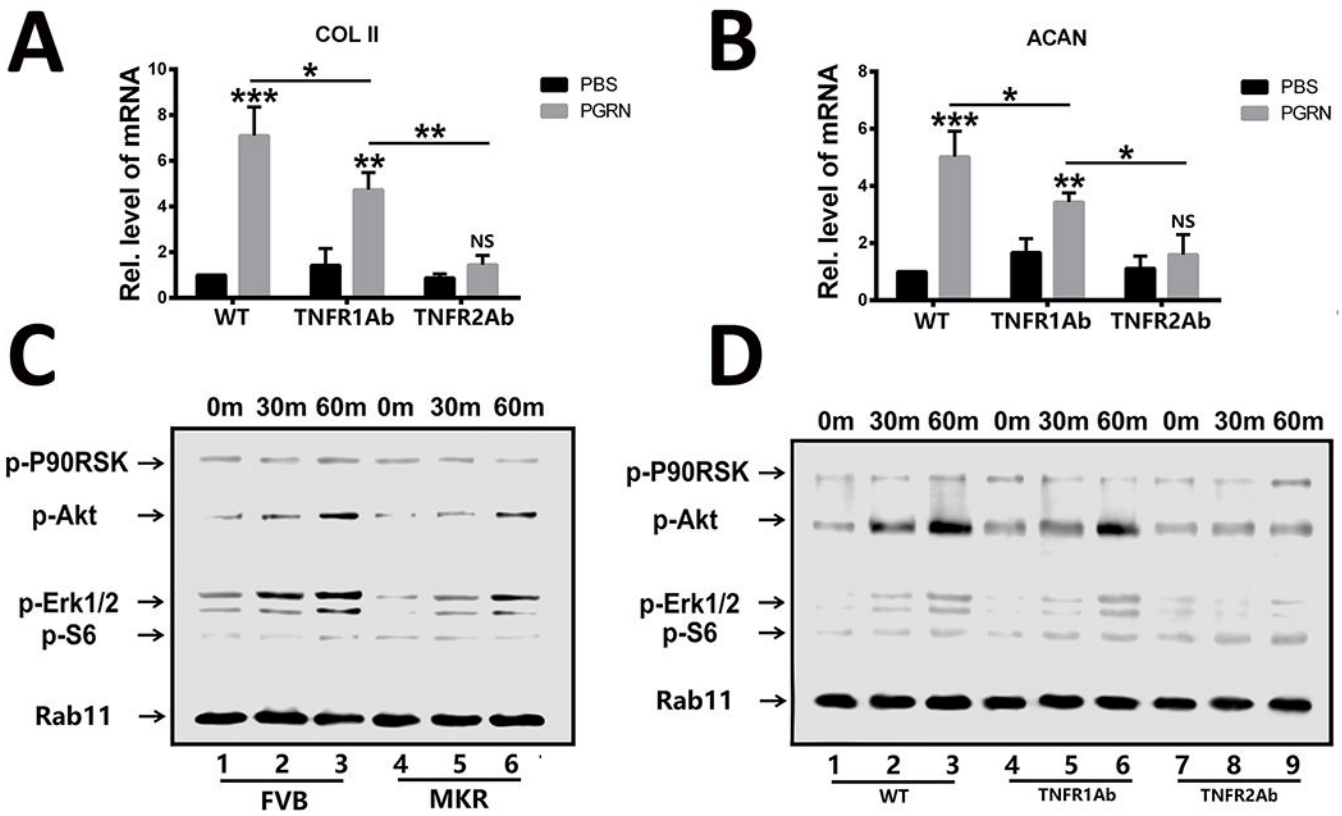

Figure.6. PGRN promotes chondrogenic gene expression in bone marrow cells from T2DM mice via TNFR2-Akt and Erk1/2 signaling in T2DM.

(**A**, **B**) Transcriptional expression of *COL2A1* (type II collagen) and *ACAN* (aggrecan) in primary bone marrow cells from MKR mice in the absence or presence of recombinant PGRN with TNFR1 or TNFR2 antibody. (**C**) Primary FVB and MKR mouse bone marrow cells were incubated with PGRN, and activation of signaling molecules were examined by cocktail antibody scanning. (**D**) Activation of the indicated signaling molecules was assayed by cocktail scanning in the presence of TNFR1 or TNFR2 antibody in primary MKR bone marrow cells. The values shown represent the mean ± standard deviation. *$p < 0.05$ and ** $p < 0.01$ vs. control group.

Table 1.

Specific primers used in the study

Gene	Forward (5′–3′)	Reverse (5′–3′)
PGRN	TGGTGGAGCAGCAAGAGCAA	CAGTGGACAGTAGACGGAGGAAA
ACAN	AATGCTGGTACTCCAAACCC	CTGGATCGTTATCCAGCAAACAGC
COL2A1	ACTAGTCATCCAGCAAACAGCCAGG	TTGGCTTTGGGAAGAGAC
IL1B	AATCTCACAGCAGCACATCA	AAGGTGCTCATGTCCTCATC
COX2	AACCGCATTGCCTCTGAAT	CATGTTCCAGGAGGATGGAG
NOS2	ACAGGAGGGGTTAAAGCTGC	TTGTCTCCAAGGGACCAGG
GAPDH	AGAACATCATCCCTGCATCC	AGTTGCTGTTGAAGTCGC